Gyroscopes in General Relativity
Istituto Nazionale di Fisica Nucleare

Ginger data analysis: data analysis for seismology, laser optimization

Simone Castellano

Main research directions:

- Data production and analysis for seismology, Gingerino sensitivity to noise from human activities
- Laser characterization, laser interference optimization
- Diagnostics

INTRODUCTION: GINGER, prototypes, the working principle

The GINGER experiment, under construction in 2024, is based on Ring Laser Gyroscopes, a particular type of interferometers, exploiting the Sagnac effect

*GINGER, Mathematics and Mechanics of Complex Systems Vol. 11 (2023), No. 2, 203–234, DOI: 10.2140/memocs.2023.11.203

***Detect* —> Earth motions: seismic events, tides, polar motions**
—> fundamental physics: Lense Thirring effect, extensions of General Relativity.

The working principle: *non reciprocity of two counter-propagating light beams inside a closed path* rotating with the Earth
Detection scheme—> beat-note produced by interference of the two counter propagating beams (Sagnac Effect)

RLG schematic view:

GINGERino @ LNGS, currently taking data ***IV.GIGS seismic station is also visible***

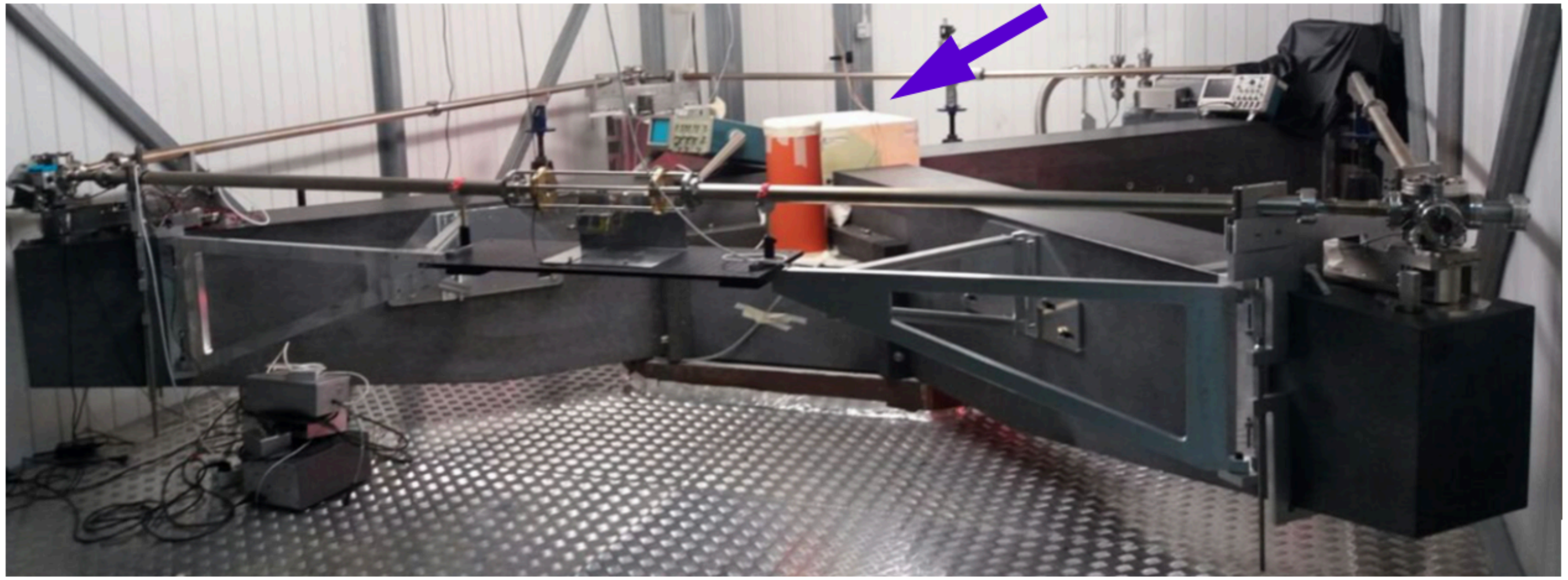

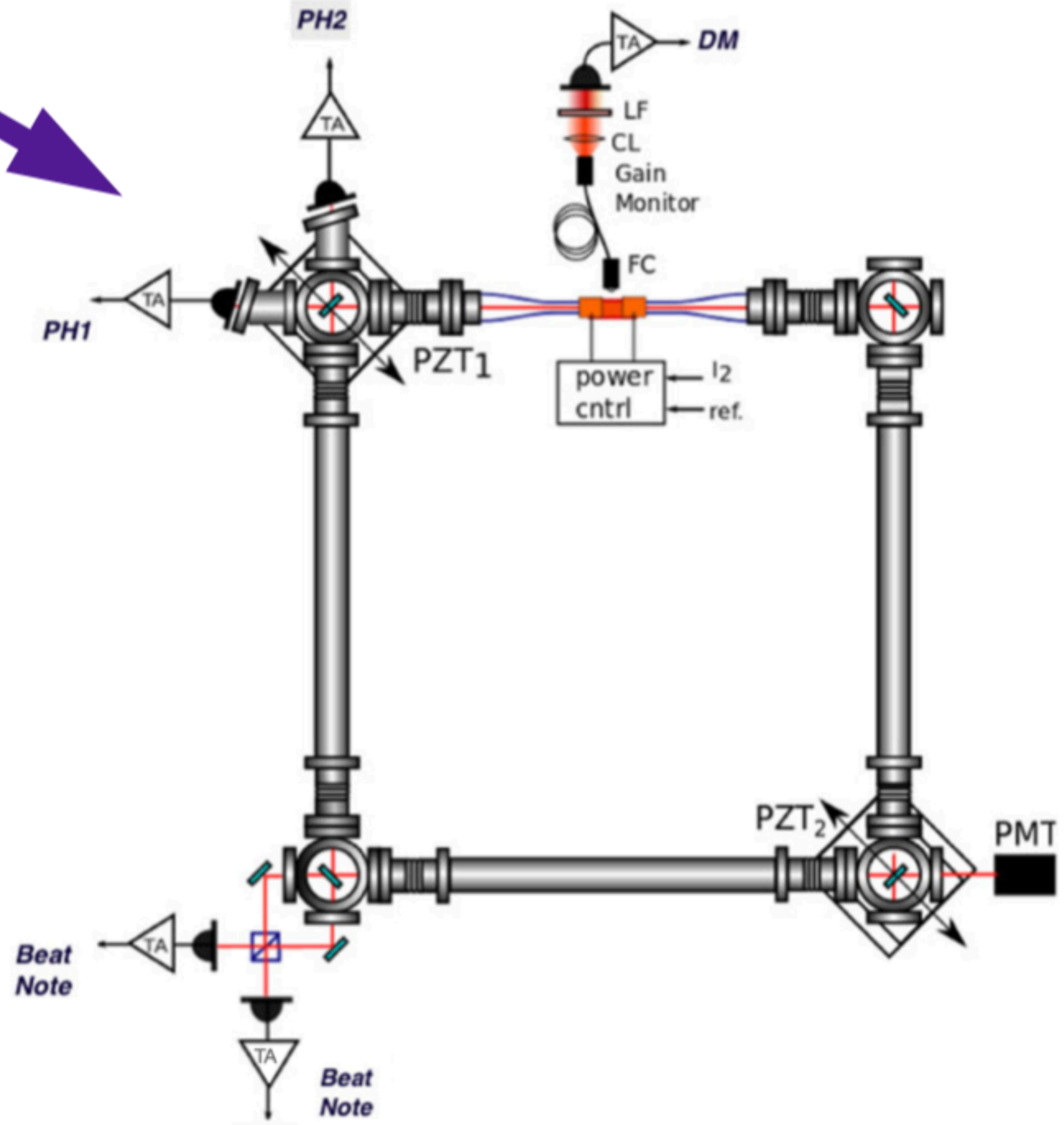

Sagnac Effect and Earth based RLG signal

Earth rotation —> the two counter-propagating cavity modes have slightly different frequency

—> ***measured beat note*** ω_m —Analysis—> ***Sagnac frequency*** ω_s

$\omega_s \propto \Omega$, rotation rate which affects the apparatus:

$$\omega_s = \frac{4A}{\lambda L}\Omega cos(\theta),$$

where: **A** is the area of the ring cavity, **L** is its perimeter, **λ** the wavelength of the light, and **θ** is the angle between the area versor of the ring and the orientation of **Ω**.

Horizontal RLG —> $\theta =$ **co-latitude**

Maximum Sagnac Signal (axis parallel to Earth rotation axis) —> $\theta = 0$

The scale factor:

$$S = \frac{4A}{\lambda L}$$

—> for GINGERino, which is horizontal within the ~mrad, the conversion factor between Hz and rad/s is:

$$S = \frac{4 \cdot 3.6^2}{633 \cdot 10^{-9} \cdot 4 \cdot 3.6} \sim 5.6872 \cdot 10^6 \; Hz/(rad/s),$$

A typical Sagnac frequency of 280.38 Hz is consistent with an Earth rotation angular velocity of ~ $7.2921 \cdot 10^{-5}$ ***rad/s, and Ring Laser gyroscope horizontal within ~mrad.***

The GP2 prototype @INFN-Pisa

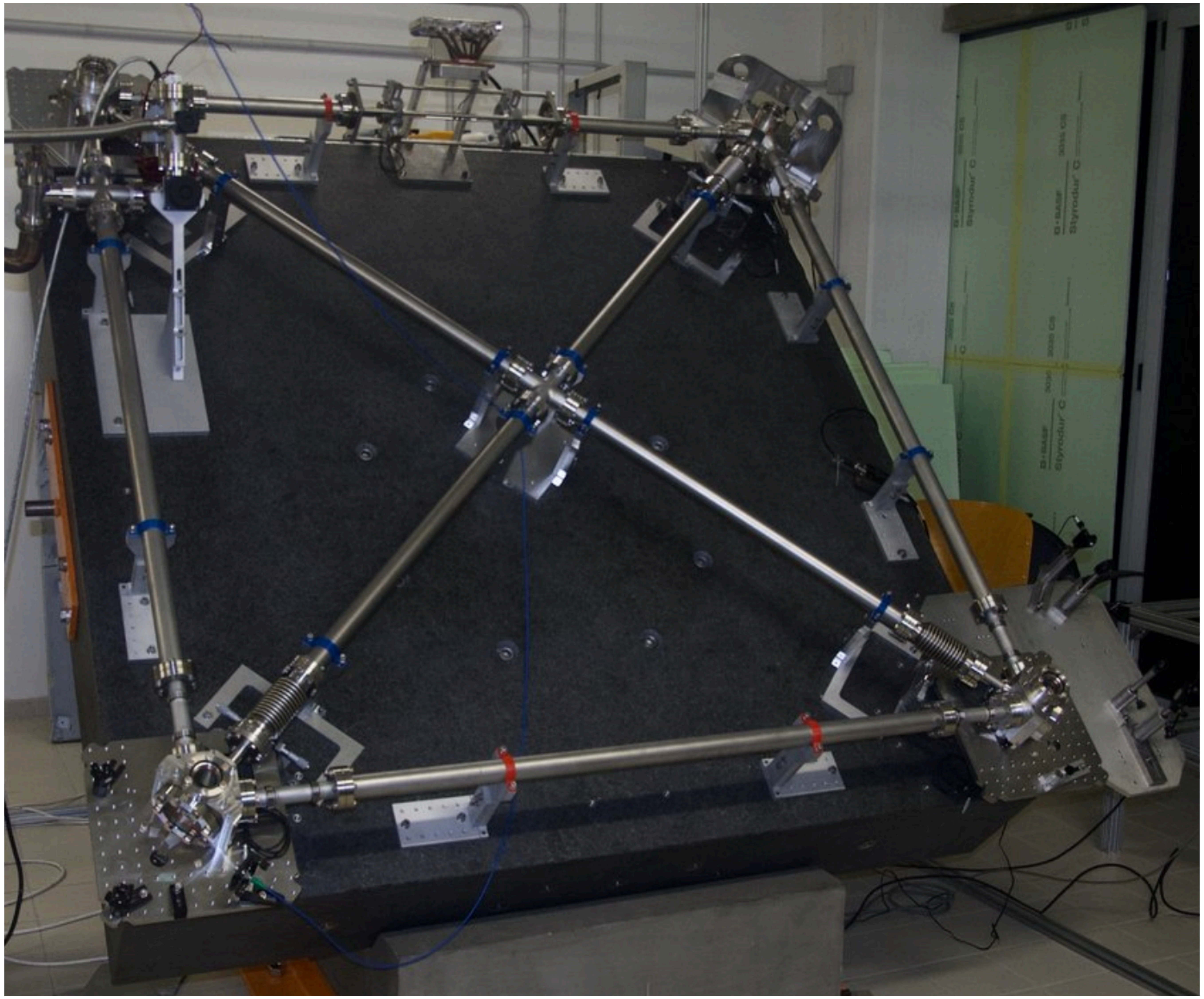

In this case, we have an RLG at the maximum Sagnac signal, and

$$S = \frac{4 \cdot 1.6^2}{633 \cdot 10^{-9} \cdot 4 \cdot 1.6} \sim 2.5276 \cdot 10^6 \; Hz/(rad/s),$$

A typical Sagnac frequency of 184 Hz is consistent with an Earth rotation angular velocity of

~ $7.2921 \cdot 10^{-5}$ ***rad/s.***

E.Maccioni et al., High sensitivity tool for geophysical applications: a geometrically locked ring laser gyroscope, Applied Optics Vol. 61, Issue 31, pp. 9256-9261 (2022) https://doi.org/10.1364/AO.469834

Analysis: Backscattering and "null shift"

Measured beat note ω_m

Taking into account:

- Backscattering (Due to mirror imperfections) → ω_{s0} **"Fast" Approximation of the Sagnac frequency**
- Laser dynamic effects (null shift), cavity losses evaluated with linear regression methods

→ ω_s **Best evaluation of the Sagnac frequency, its implementation is in progress**

ω_{s0} Is the "fast" approximation of ω_s : the 1st order term of ω_s , obtainable directly from raw data:

$$\omega_{s0} = \frac{1}{2}\sqrt{\frac{2I_{S1}I_{S2}\omega_m^2 cos(2\epsilon)}{I_1 I_2} + \omega_m^2} + \frac{\omega_m}{2},$$

Where:

- $I_{1,2}$ are the DC level of the mono-beam signals
- ω_m is the measured beat note
- $I_{S1,S2}$ are the amplitudes of the mono-beam signals demodulated at the Sagnac frequency
- ϵ is the phase difference between the 2 mono-beam signals

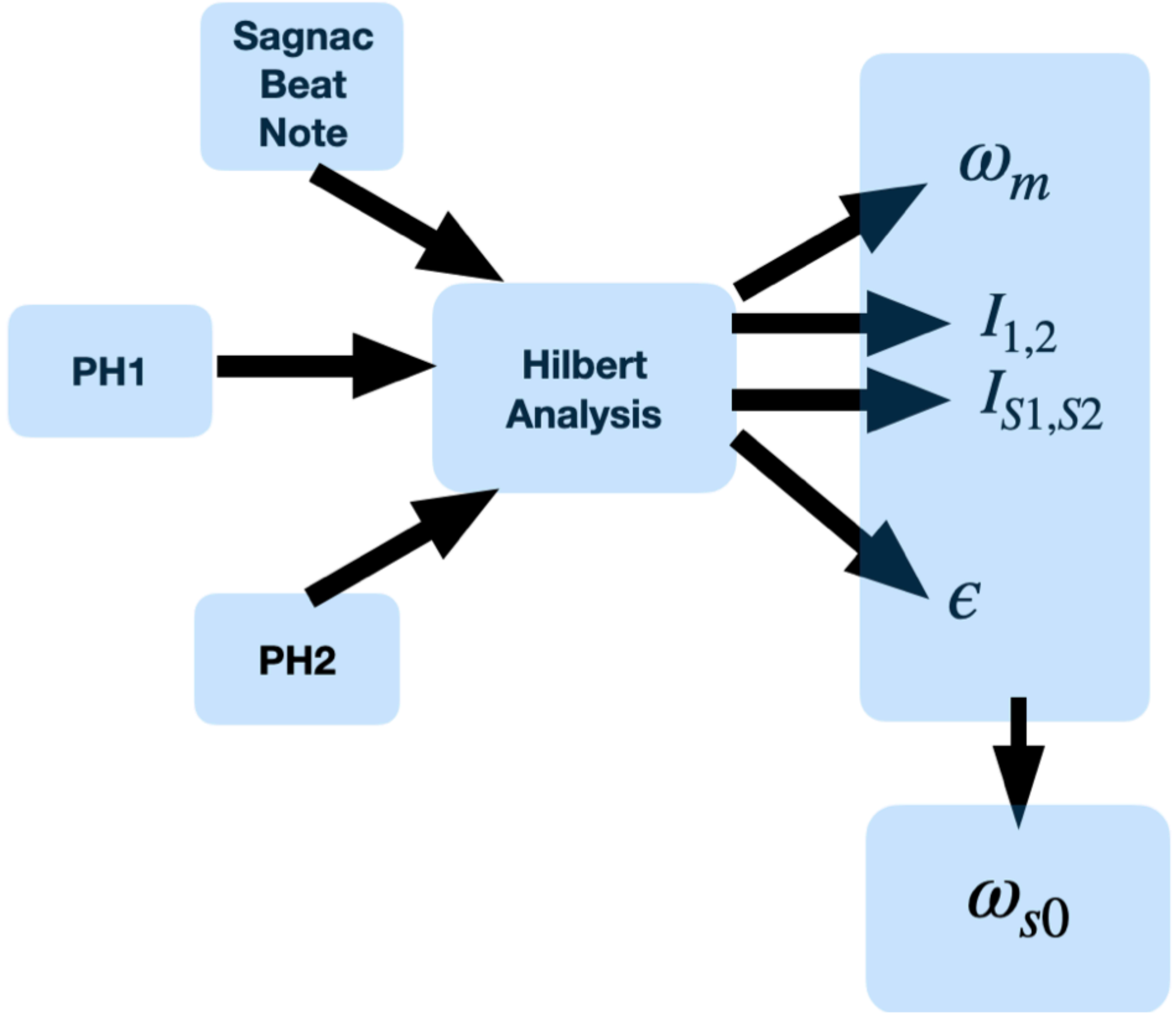

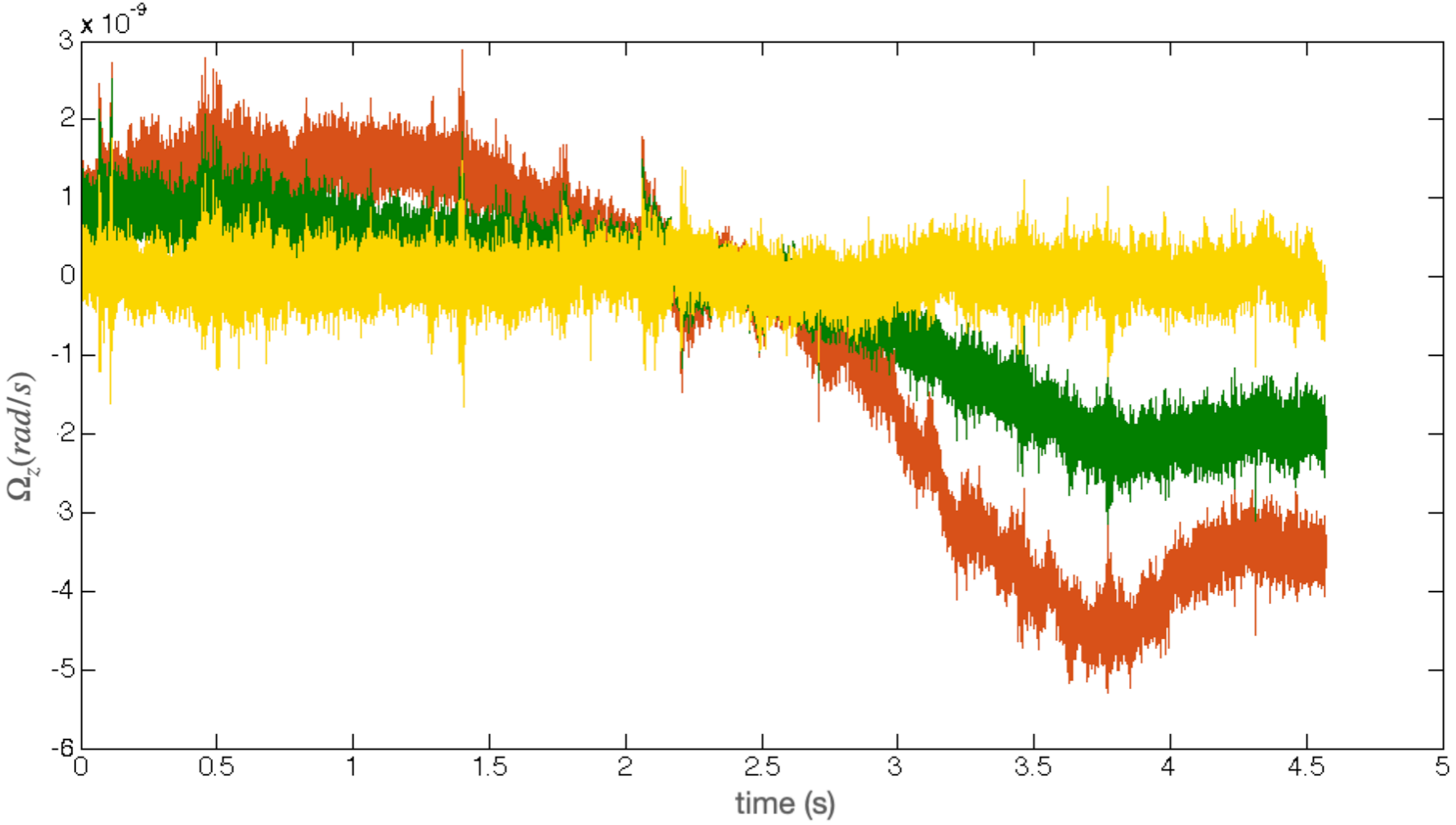

Comparison of ω_m(red), ω_{s0}(green), and ω_s(yellow) on a small portion of data.

Data production and analysis for seismology

For seismology analysis, ω_{s0} is utilized:

- *100 Hz bandwidth; 100 Hz decimated data*
- *DAQs: "Centaur" (2 kHz), "PXI" (5 kHz)*
- *Delay possibly as short as 1 s*
- *Frequency range: from 10mHz up to 100Hz, in this frequency range $\omega_{s0} \simeq \omega_s$*
- *2023 data were provided for upload on EIDA*
- *A plugin is soon implemented for real time data production, in collaboration with A.Govoni*
- *Previous years to be analyzed and provided*

Turkey event of 2023-2-6, 1:17 UTC. T(0)= '06-Feb-2023 01:00:00'

(For imaging purposes, GINGERino data are filtered here with a bp-filter ±10 Hz around the Sagnac frequency)

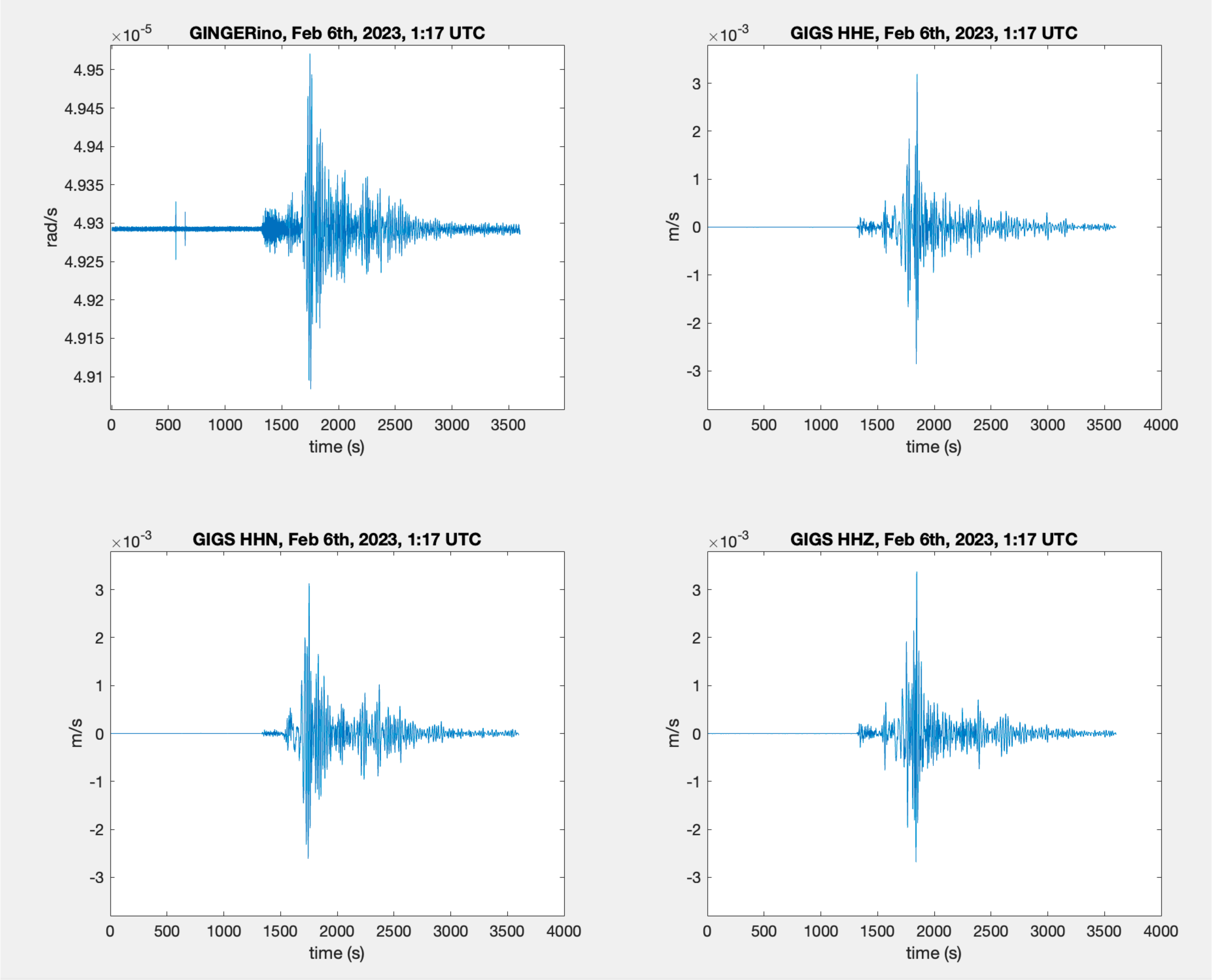

GIGS + GINGERino becomes a 4C seismic station:

- **correspondence between transverse acceleration a_t and ω_z, in this case represented by ω_{s0} : $a_t = 2c\omega_z$, where c is the phase velocity of transverse polarized waves —> estimation of phase velocity, back azimuth**
- **GINGER will be a 6C seismic station (importance of being colocated with GIGS seismometer)**

18TH WORLD CONFERENCE ON EARTHQUAKE ENGINEERING
WCEE2024
MILAN
MILAN, ITALY
30TH JUNE - 5TH JULY 2024
www.wcee2024.it

4C EARTHQUAKE RECORDINGS AT GRAN SASSO FOR A BETTER COMPREHENSION OF GROUND MOTION

D. Famiani[1], G. De Luca[2], A. Govoni[1], A. Mercuri[1]

G. Carelli[3,4], S. Castellano[4,5], A. D. V. Di Virgilio[4], E. Maccioni[3,4], P. Marsili[3,4]

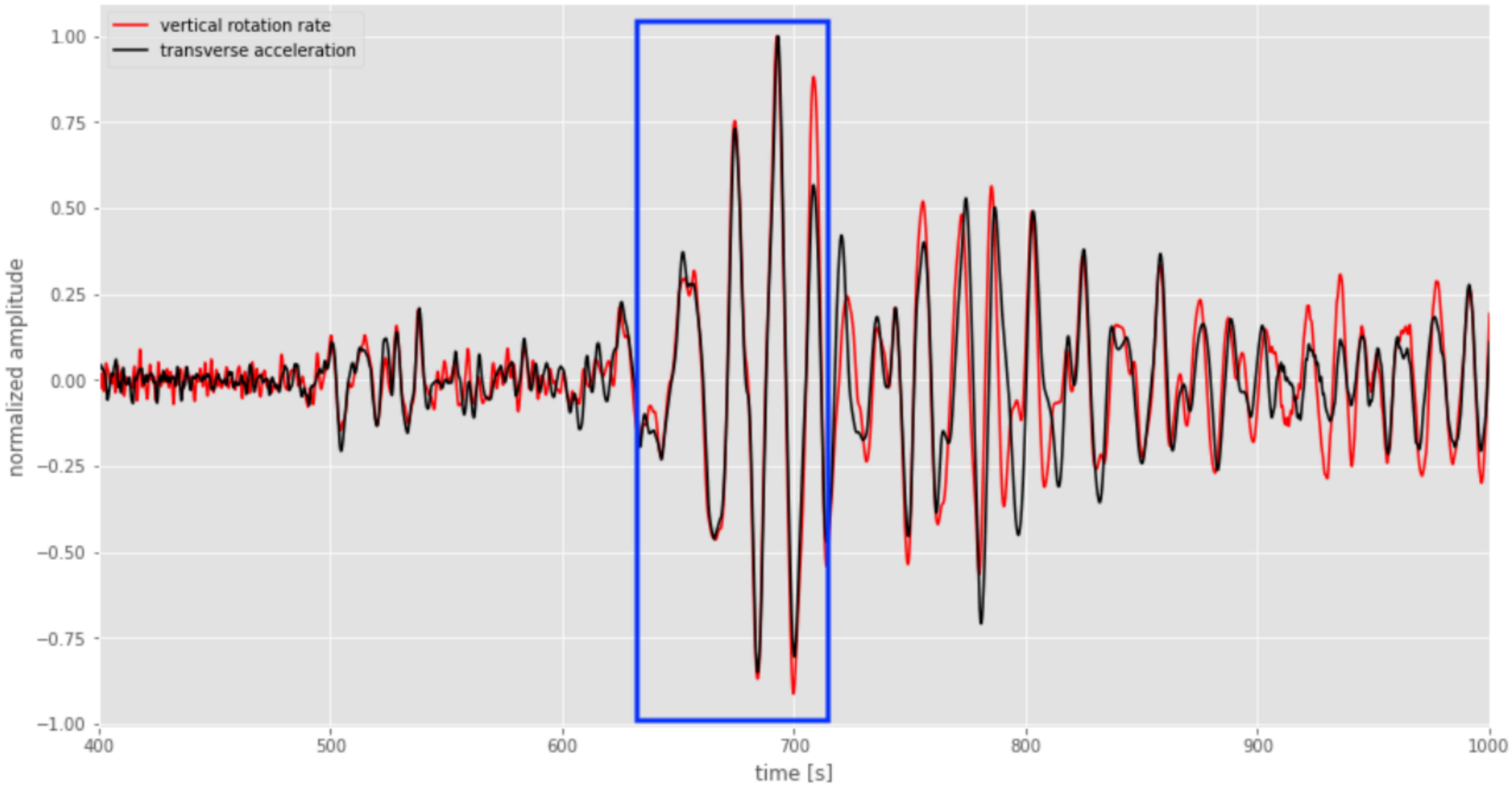

Gingerino sensitivity to noise from human activity:

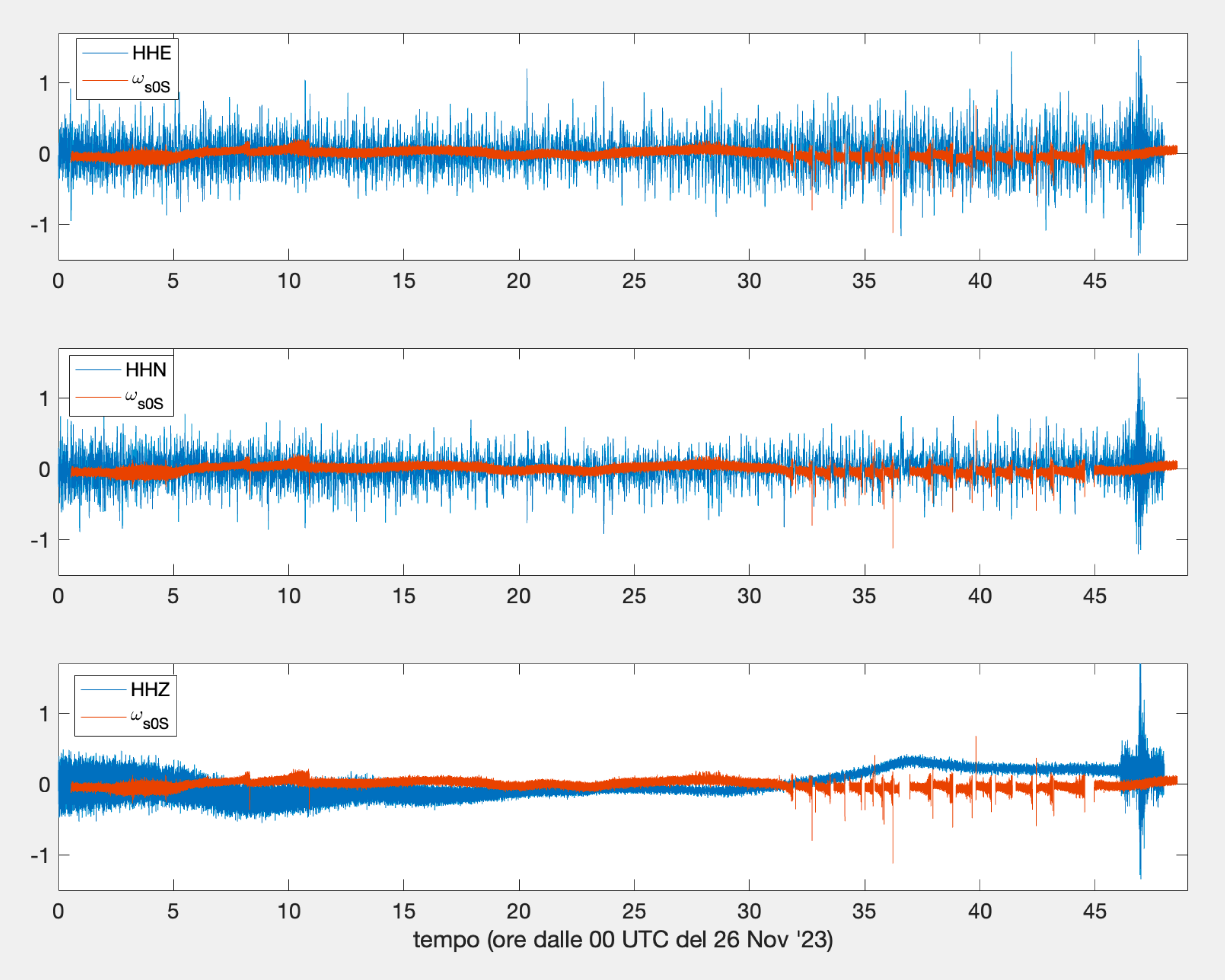

Gingerino appears to be sensitive to local environmental background:

Data from November 26th and 27th, GIGS channels Gingerino, decimated down to 5 Hz.
Gingerino data were selected "good", so they are missing in presence of "split modes".

The hypothesis is that laser works in "split mode" because of the vibrations from human activity @LNGS (i.e. Darkside installation road works), in fact this is visible during day time and not i.e. November 26th, which was Sunday.

Laser characterization and interference optimization (data utilized in this work are from GP2 @ INFN-Pisa)

Data selection: fringe contrast

Factorization of Fringe Contrast: models

Measurements of beams polarization inside and outside the laser cavity

Ring laser optimization

Measurement of cavity non planarity, beams off-axis

Typical disturbances and data quality

Disturbances
- Mode jumps → very fast spikes, affecting data for a few seconds
- Split modes → disturbances that last for hours, but can be eliminated or reduced by geometry control or software procedures to restore the correct operation

In figure, the **measured beat note frequency** ω_m , expressed in terms of angular velocity;
its mean value is subtracted, **disturbance effects** are visible at the **nano-rad/s** level (equivalent to ~ **a few mHz - 10 mHz**).

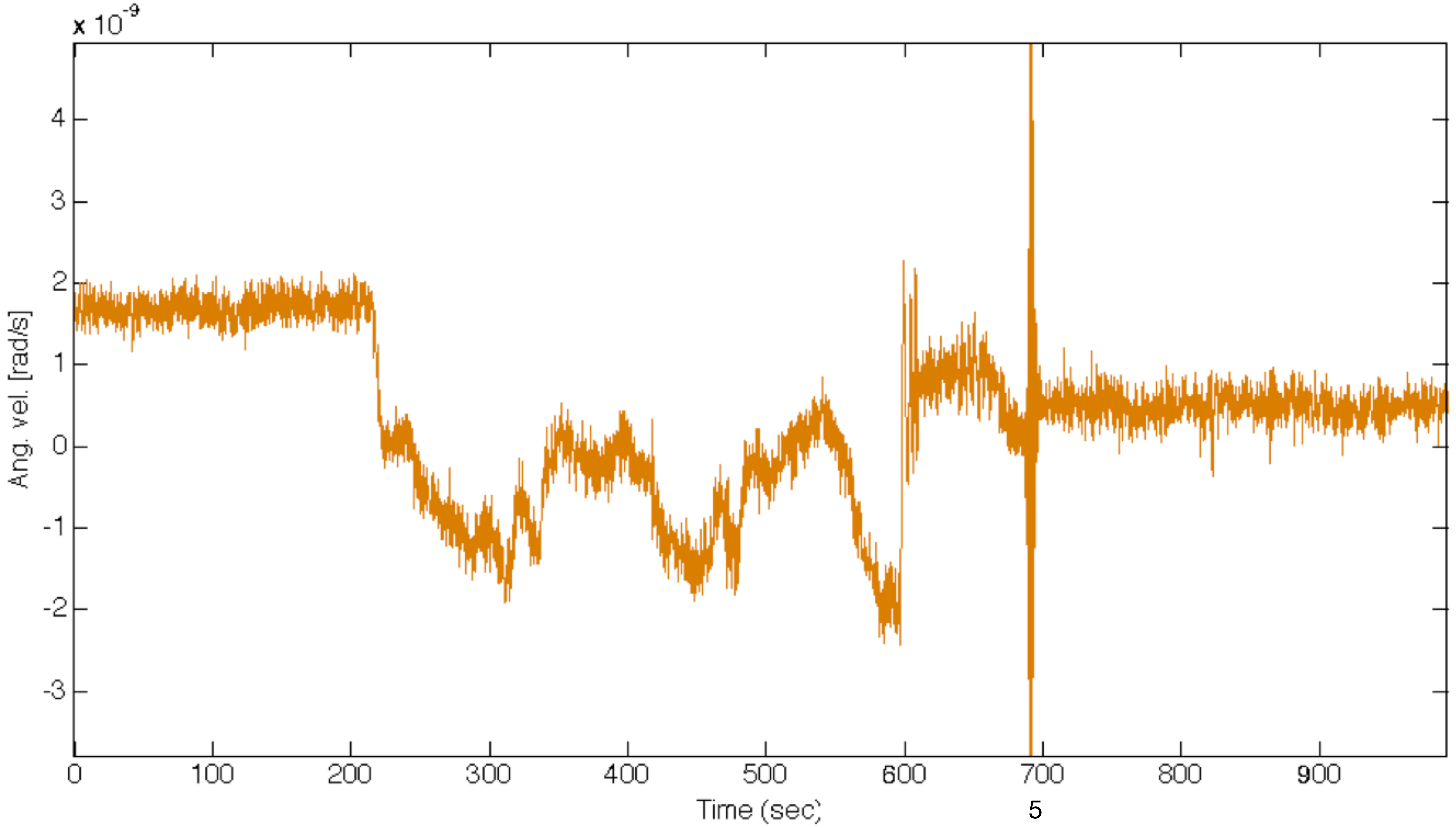

Data selection

One of the most utilized parameters for data selection is Fringe Contrast:

$$C = \frac{I_{max} - I_{min}}{I_{max} + I_{min}},$$

where I_{max} and I_{min} are the local intensity maxima and minima of the beat note signal.
From light interference:

$$I_{min} = I_1 + I_2 - 2 \cdot \sqrt{I_1 \cdot I_2} \cdot \eta_{vis},$$

$$I_{max} = I_1 + I_2 + 2 \cdot \sqrt{I_1 \cdot I_2} \cdot \eta_{vis}$$

Therefore:

$$C = \frac{I_{max} - I_{min}}{I_{max} + I_{min}} = \frac{2 \cdot \sqrt{I_1 \cdot I_2}}{I_1 + I_2} \cdot \eta_{vis}$$

Where η_{vis} is a “visibility” parameter, which we will factorize as a product of 2 contributions:

$$\eta_{vis} = \eta_{geom} \cdot \eta_{pol},$$

η_{geom} from geometrical superimposition of two gaussian beams, and η_{pol} from the interaction between 2 polarization states

Example of data selection utilizing Fringe Contrast

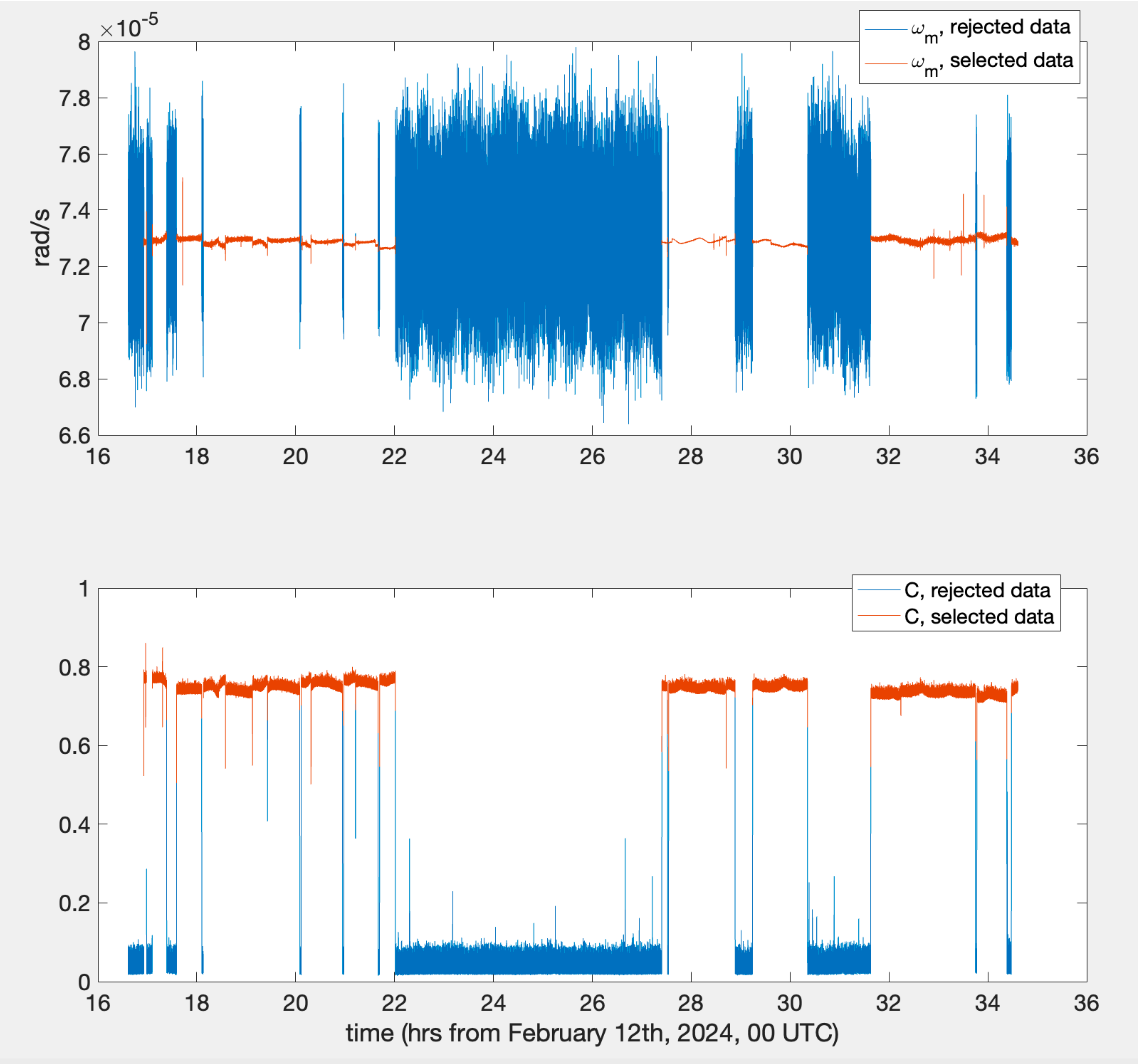

Data selection utilizing fringe contrast is shown, on a dataset of ~20 hours.

Below, contrast is shown, it clearly indicates when the laser is creating a good interference signal.

Above, in correspondence of a valid fringe contrast value, the Earth rotation rate value is well reproduced, the standard deviation of the measured rotation rate is an indicator of data quality

Low duty cycle (GP2 is situated in a disturbed environment)

Model for the geometrical term η_{geom}

If we consider the beams off-axis as the only contribution to Contrast, we have:

$$\eta_{geom} = \frac{I_{max} - I_{min}}{I_{max} + I_{min}}$$

Let us derive I_{max} and I_{min} as function of the beams off-axis "k", where "k" is expressed in units of $\sigma \cdot \sqrt{2}$ of the gaussian beam, i.e. the radius where the fields intensity is $1/e^2$ of its on-axis value.

$$I_{max} = \frac{1}{2\pi} \int_{-\infty}^{+\infty} \int_{-\infty}^{+\infty} (e^{-[(x+k)^2+y^2]} + e^{-[(x-k)^2+y^2]})^2 \, dxdy$$

$$I_{min} = \frac{1}{2\pi} \int_{-\infty}^{+\infty} \int_{-\infty}^{+\infty} (e^{-[(x+k)^2+y^2]} - e^{-[(x-k)^2+y^2]})^2 \, dxdy$$

$$\longrightarrow \quad \eta_{geom} = e^{-2k^2} \quad \longrightarrow$$

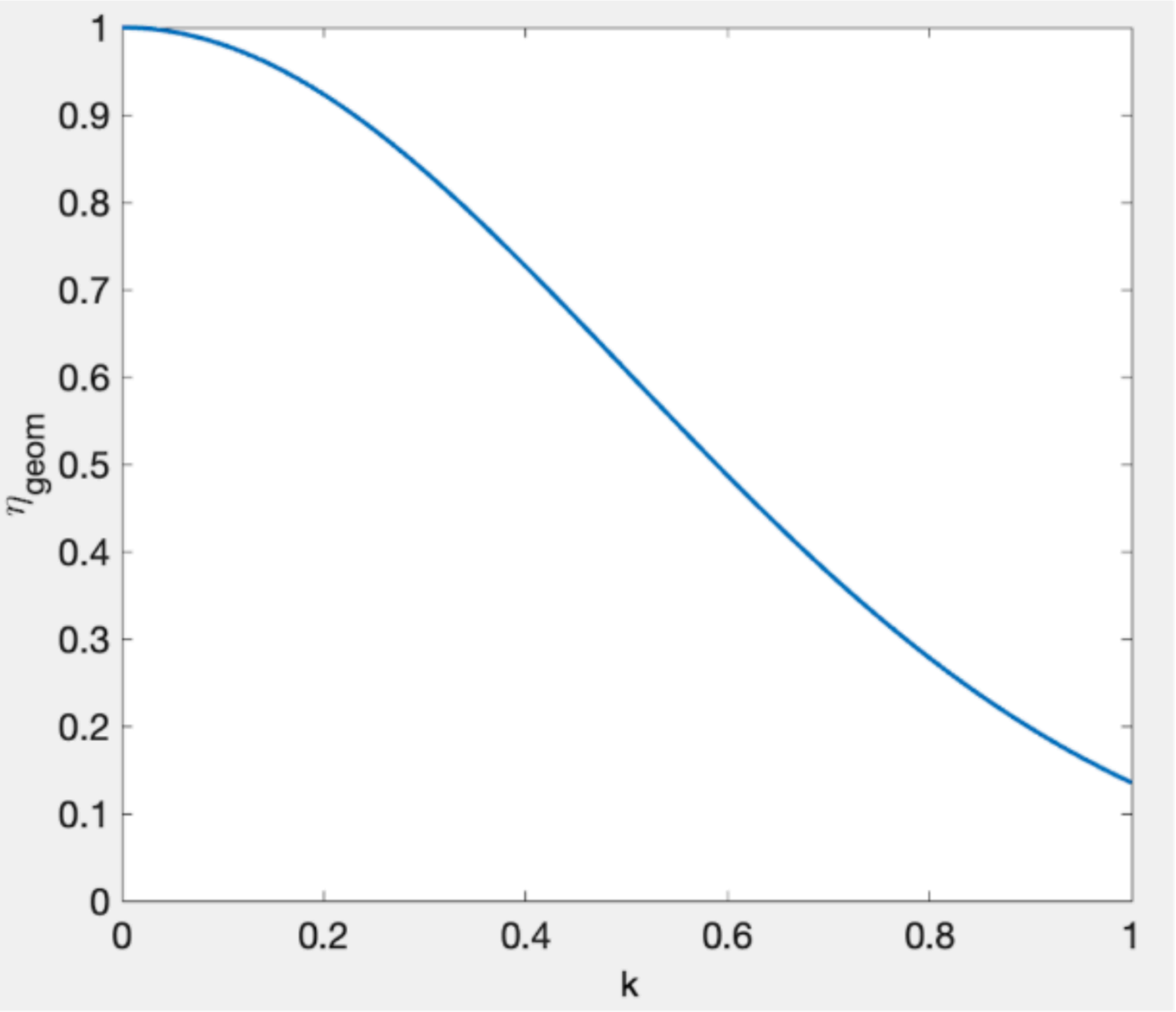

Model for the polarization term η_{pol}

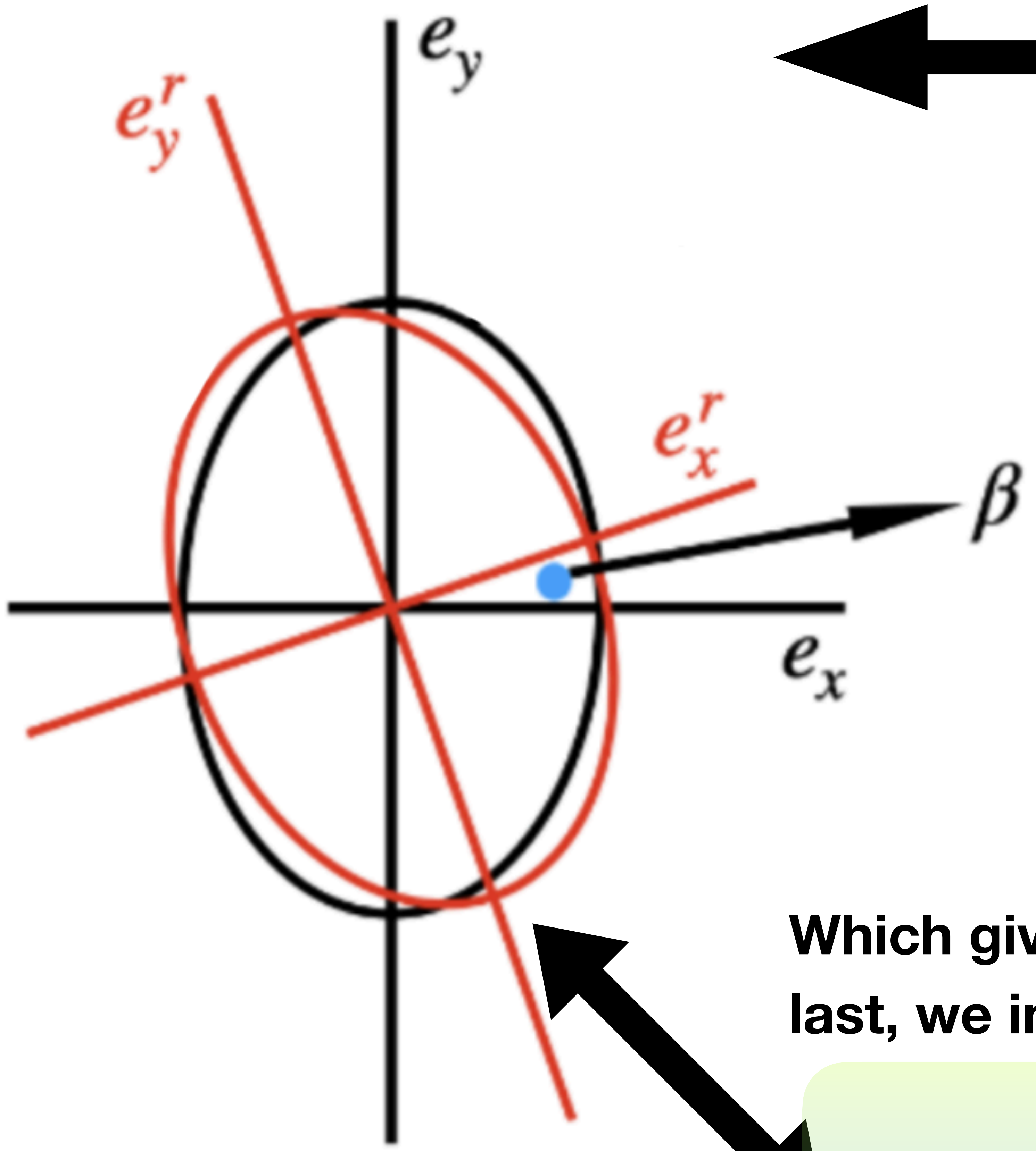

The most general situation that can be encountered in 2 interfering beams' polarization: elliptical polarization states, with some non-zero angle between the two.

Let us derive η_{pol} for such case.
For the circular case we have:

$$\eta_{pol} = |e_L \cdot e_L^*| = \frac{1}{2}|(e_x + ie_y)\cdot(e_x - ie_y)| = \frac{1}{2}(e_x^2 + e_y^2) = 1$$

If we turn circular into elliptical polarization states, we have:

$$\eta_{pol} = \frac{1}{2}|(ae_x + ibe_y)\cdot(ae_x - ibe_y)| = \frac{1}{2}(a^2e_x^2 + b^2e_y^2) = \frac{1}{2}(a^2 + b^2) = 1,$$

Which gives us a normalization condition for the semi axes of the polarization ellipse. If, at last, we introduce a β angle between the 2 polarization ellipses, we obtain:

$$\eta_{pol} = \frac{1}{2}|(ae_x + ibe_y)\cdot(ae_x^r - ibe_y^r)| = \sqrt{cos^2(\beta) + a^2b^2 \cdot sin^2(\beta)},$$

with "a" and "b" representing the polarization ellipse semi axes

In case a = 0 or b = 0 we obtain linear polarization states.

Measurement of the mono-beams polarizations

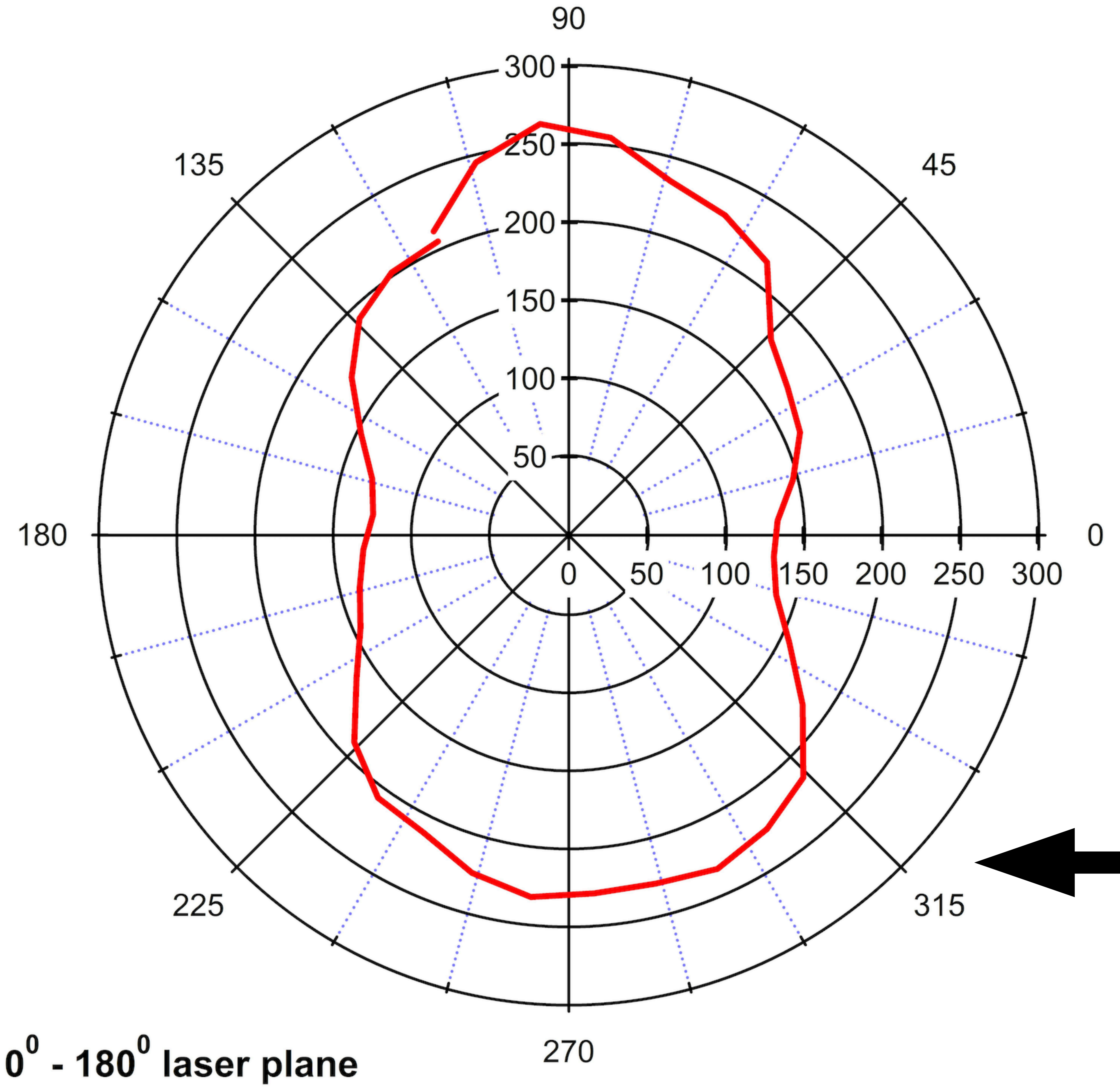

0^0 - 180^0 laser plane

A dedicated measurement of the GP2 mono-beams polarization states was performed:

- **a full reconstruction of the polarization ellipse from the intensity as a function of the polarizer's angle**

- **By means of a polarizer and a photodiode**

- **Procedure fully described in:** Ramonika Sengupta, Brijesh Tripathi, and Asha Adhiya, "Explicit Reconstruction of Polarization Ellipse using Rotating Polarizer", arXiv:2211.15244

- **the resulting intensity polar graph (left) shows a peanut shape with axes ratio 2:1, indicating ellipse axes ratio ~1.4/1**

- **Major axis is CCW rotated wrt the perpendicular to the laser plane of an angle $\phi' = (44 \pm 17)$ mrad**

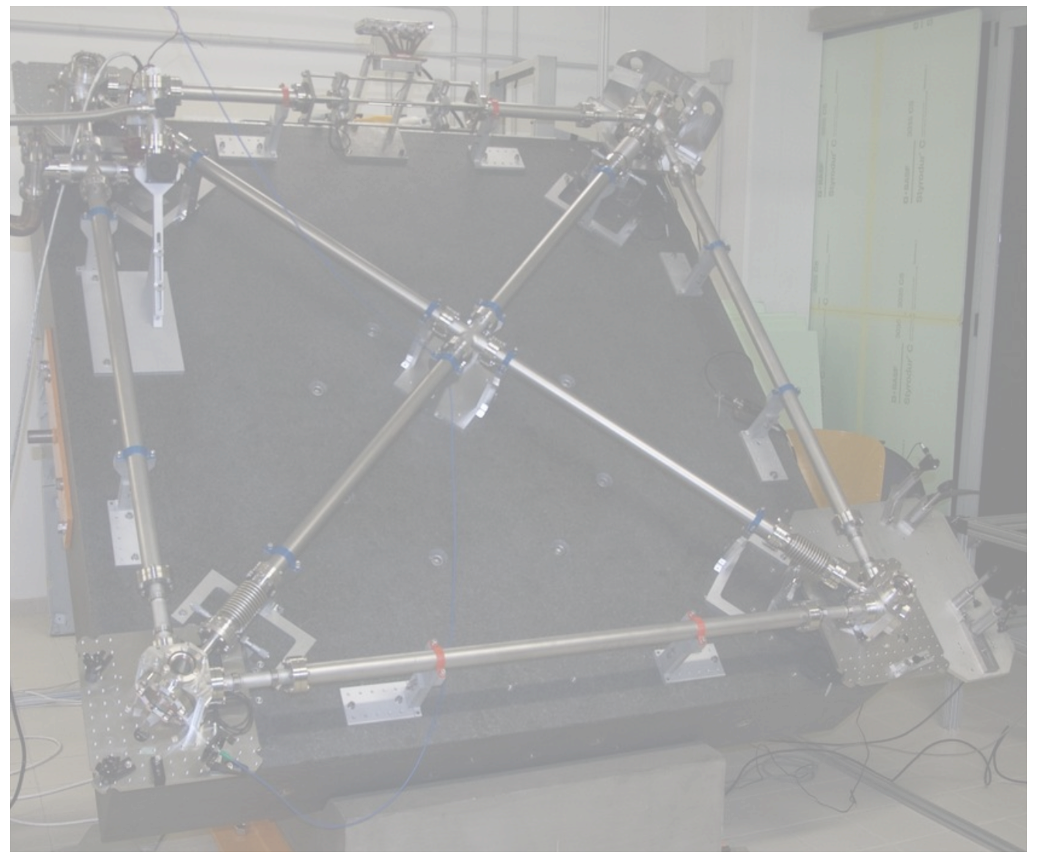

GP2 @INFN-Pisa Experimental setup

Measured polarization ellipse outside the cavity —> inferring polarization states circulating inside the cavity

(Procedure fully described in: H.R. Bilger, G.E. Stedman and P.V. Wells, "Geometrical dependence of polarisation in near-planar ring lasers", OPTICS COMMUNICATIONS (1990) Vol.80, n.2, Pages 133-137)

Measurement of the angular birefringence:

- **measurement with a dedicated setup on a test mirror, belonging to the same mounted on GP2.**
- **A linearly polarized He-Ne beam (632.8 nm) is sent on the mirror at 45° angle, and the induced polarization is measured by means of a polarizer.**
- **—> birefringence $\chi = (11 \pm 1)$ mrad**

For the same test mirrors, we measured values of the transmission coefficients T_s and T_p for S and P polarization states:

$$t_s/t_p = (T_s/T_p)^{1/2} = 0.062 \pm 0.002$$

—> anisotropy $\delta = 90 \pm 10$ ppm
—> calculation of non-planarity is performed according to the model with $\delta \ll \chi$

$$\alpha \simeq \phi' \cdot \chi \frac{t_s}{t_p} \cdot \sqrt{2} \simeq (43 \pm 15)\mu rad$$

$$\frac{E_p}{E_s} = tan(\phi) \simeq \phi = \frac{\alpha}{\chi}\frac{1}{\sqrt{2}} \simeq 0.0028$$

Cavity:

- **Non-planarity**
- **Beams polarization inside**

Interference of beams with linear and elliptical polarization states: comparisons and results.

GP2 @INFN-Pisa Experimental setup

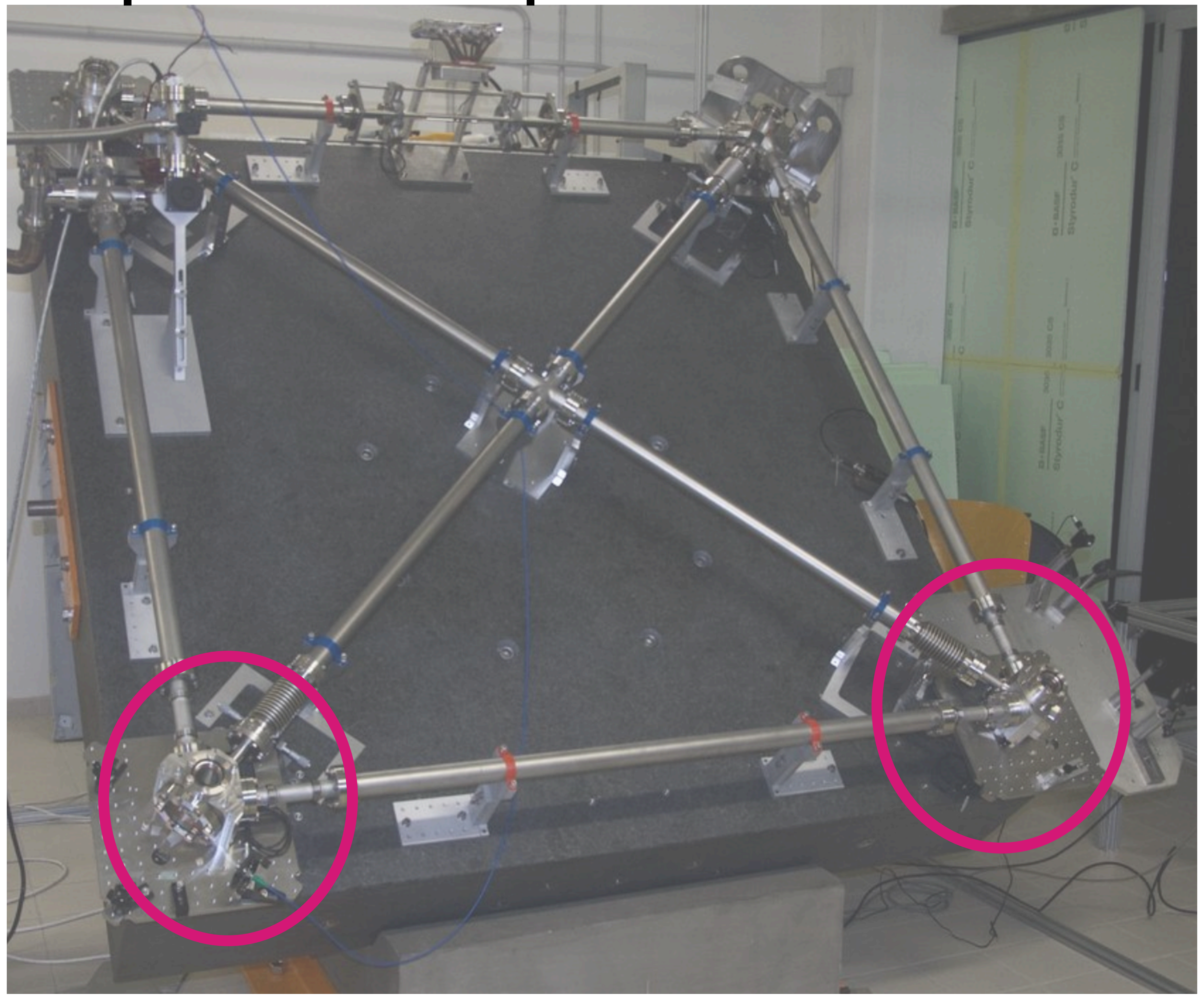

Measured beat note signals acquired at 2 different corners of the RLG at the same time:

—> any differences can be ascribed only to different polarization states.

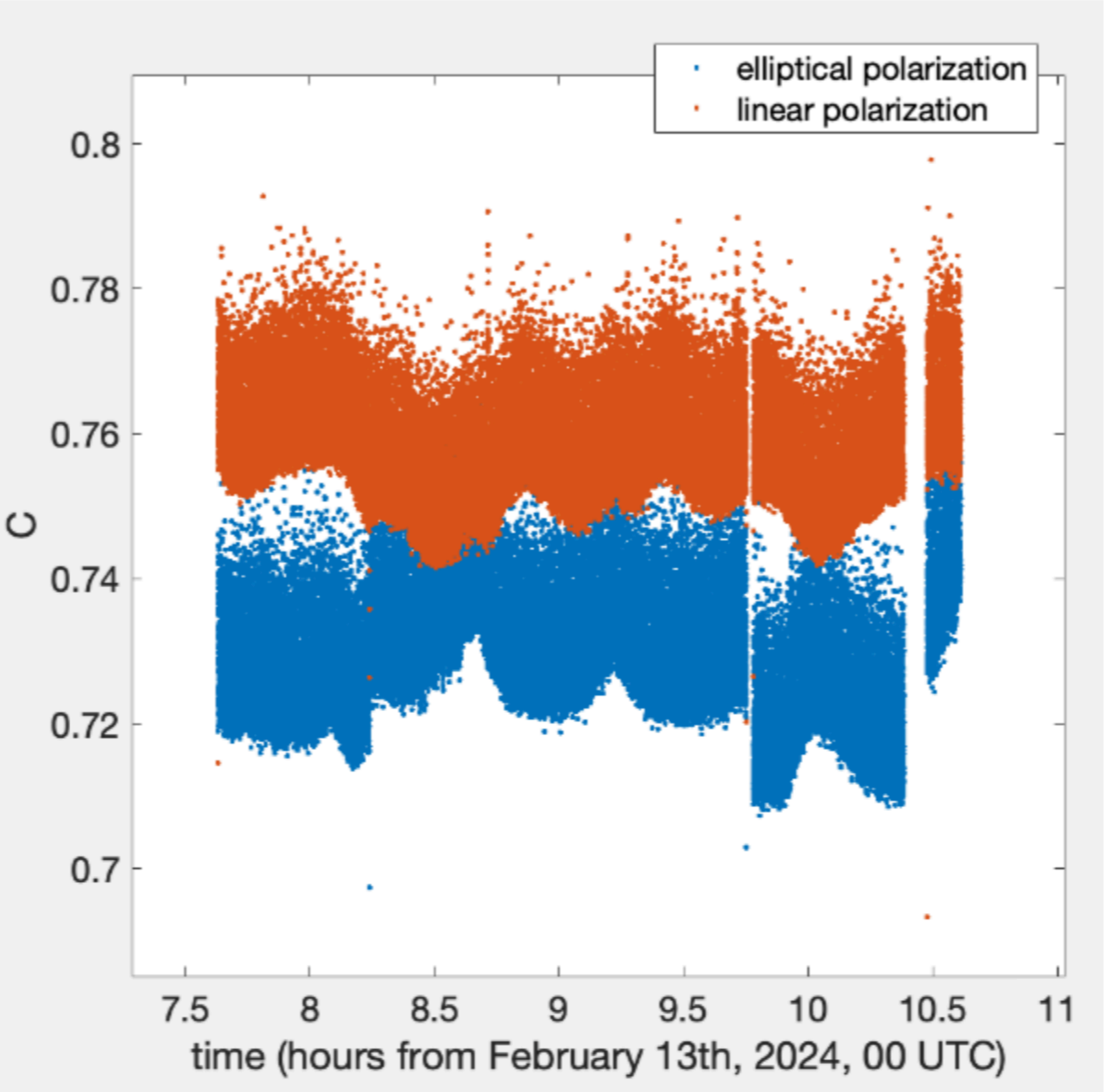

Difference in Contrast, in case of interference between beams with elliptic (a/b~1.4, blue) and linear (orange) polarization states.

contribution to contrast for linear polarization states and for elliptical states, with a/b ~ 1.4

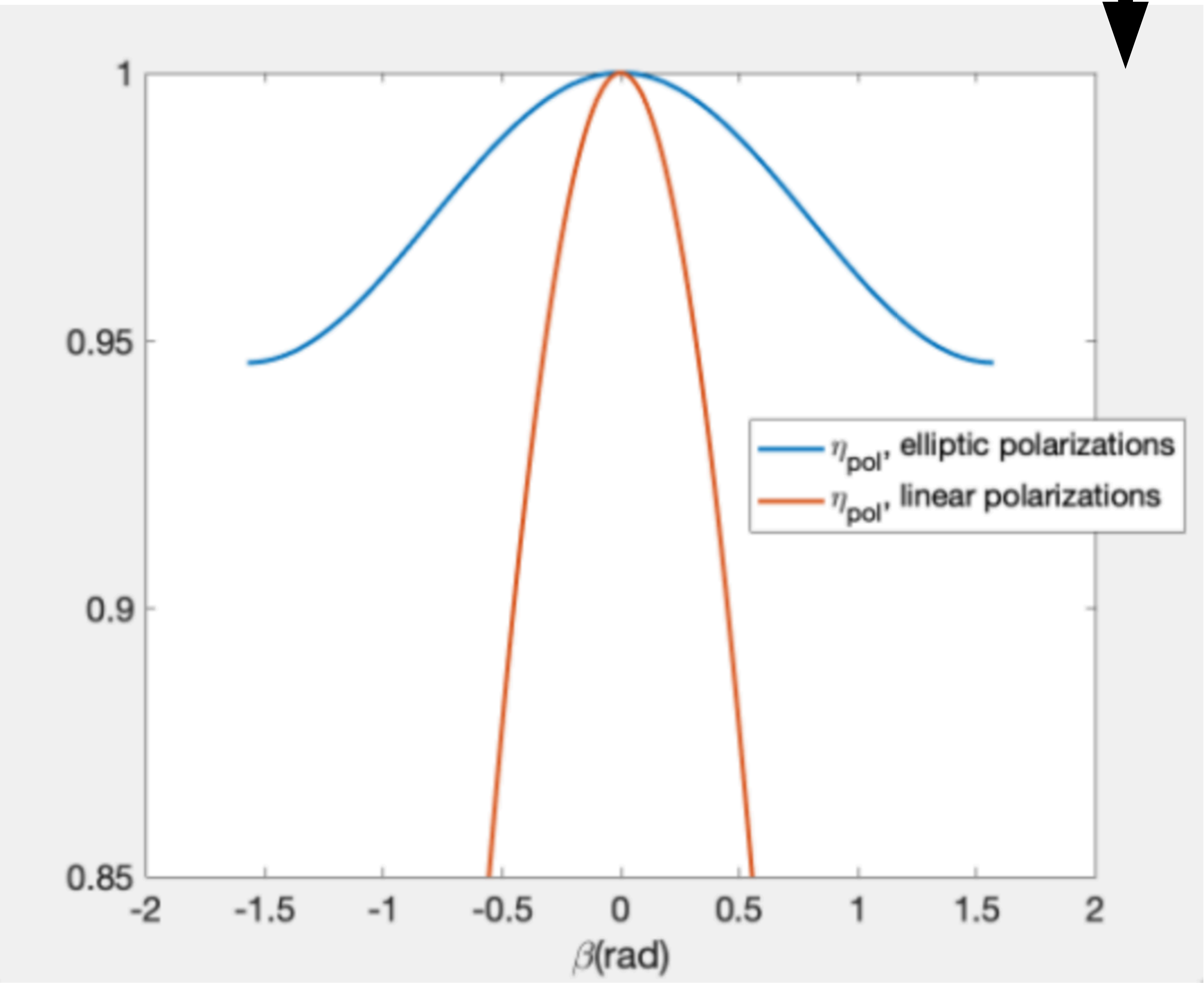

Effort in order to obtain equally polarized interfering beams, detail of the data taking in the 2 lower corners of GP2

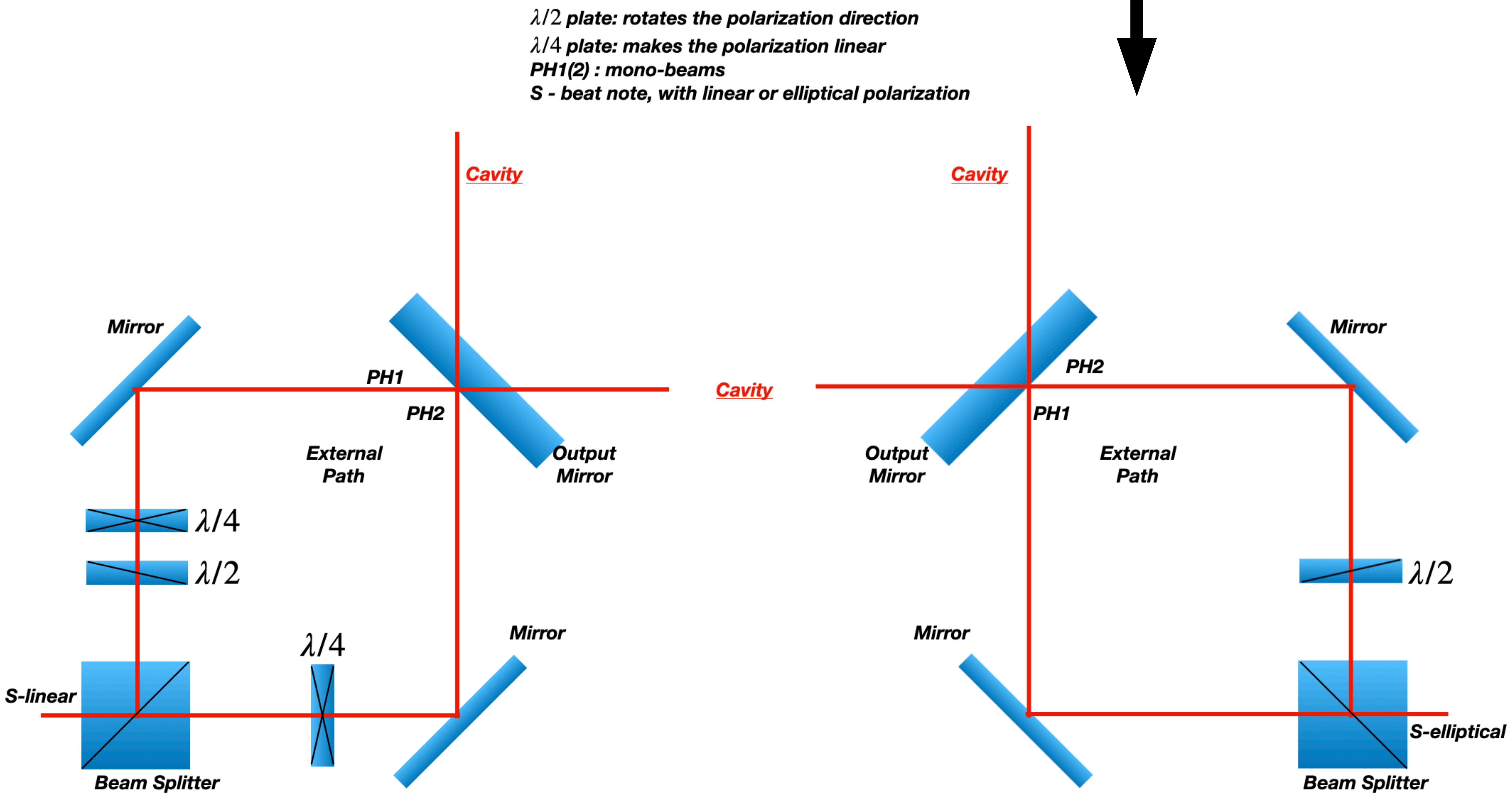

The behavior of contrast may be explained if we look at the model for η_{pol}

When we have beams with linear polarization, we can use the $\lambda/2$ plate rotation with a higher sensitivity, in order to maximize η_{pol}

If we look at Contrast and ω_m parameters:

- Contrast has higher mean value and lower std deviation, if we work with linear polarization states in the interfering beams

- **The ω_m standard deviation (table below) also confirms that, working with linearly polarized beams, the interference obtained gives better performances. This is a measurement of the signal-to-noise ratio.**

Polarizations	$\mu(contrast)$	$\sigma(contrast)$	$\sigma(\omega_m/2\pi)(Hz)$
Linear	0.761	0.0121	0.259
Elliptic	0.743	0.0134	0.265

Measurement of the beams off-axis

Utilizing data from linearly polarized beams ($\eta_{pol} \simeq 1$), we can calculate η_{geom}, hence the beams off-axis in units of a (model described in slide 15):

$$C = \frac{2 \cdot \sqrt{I_1 I_2}}{I_1 + I_2} \cdot \eta_{geom}$$ **—> a**

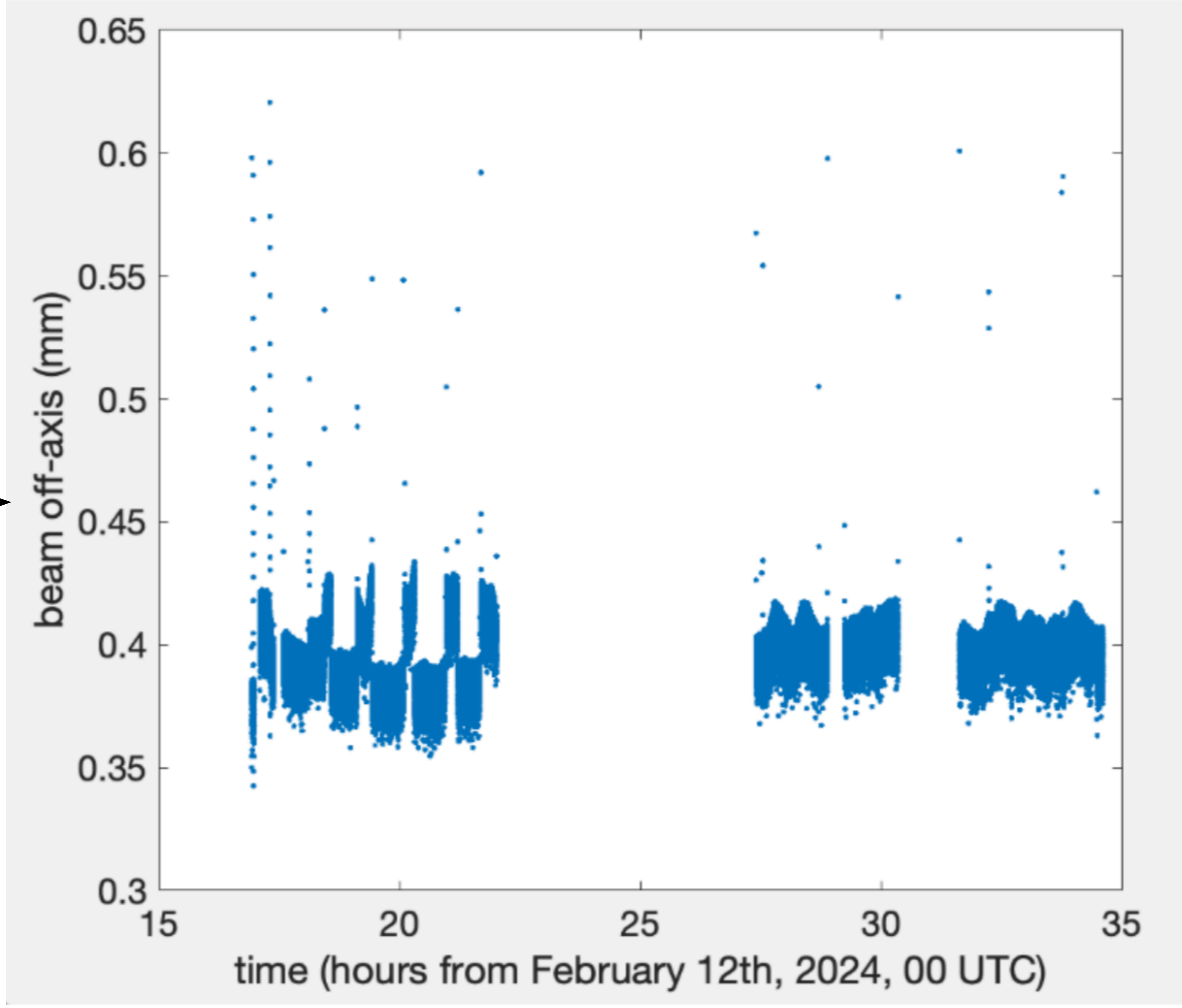

The beam gaussian profile was registered by using a webcam Encore EN-WB-UHD01.

$r = \sigma\sqrt{2} = 0.54 \pm 0.05$ **mm,**

$d = 2 \cdot a \cdot r$

Propagating the error on a and r, d = 0.40 ± 0.0.7 mm

Diagnostics

Double beat note signal

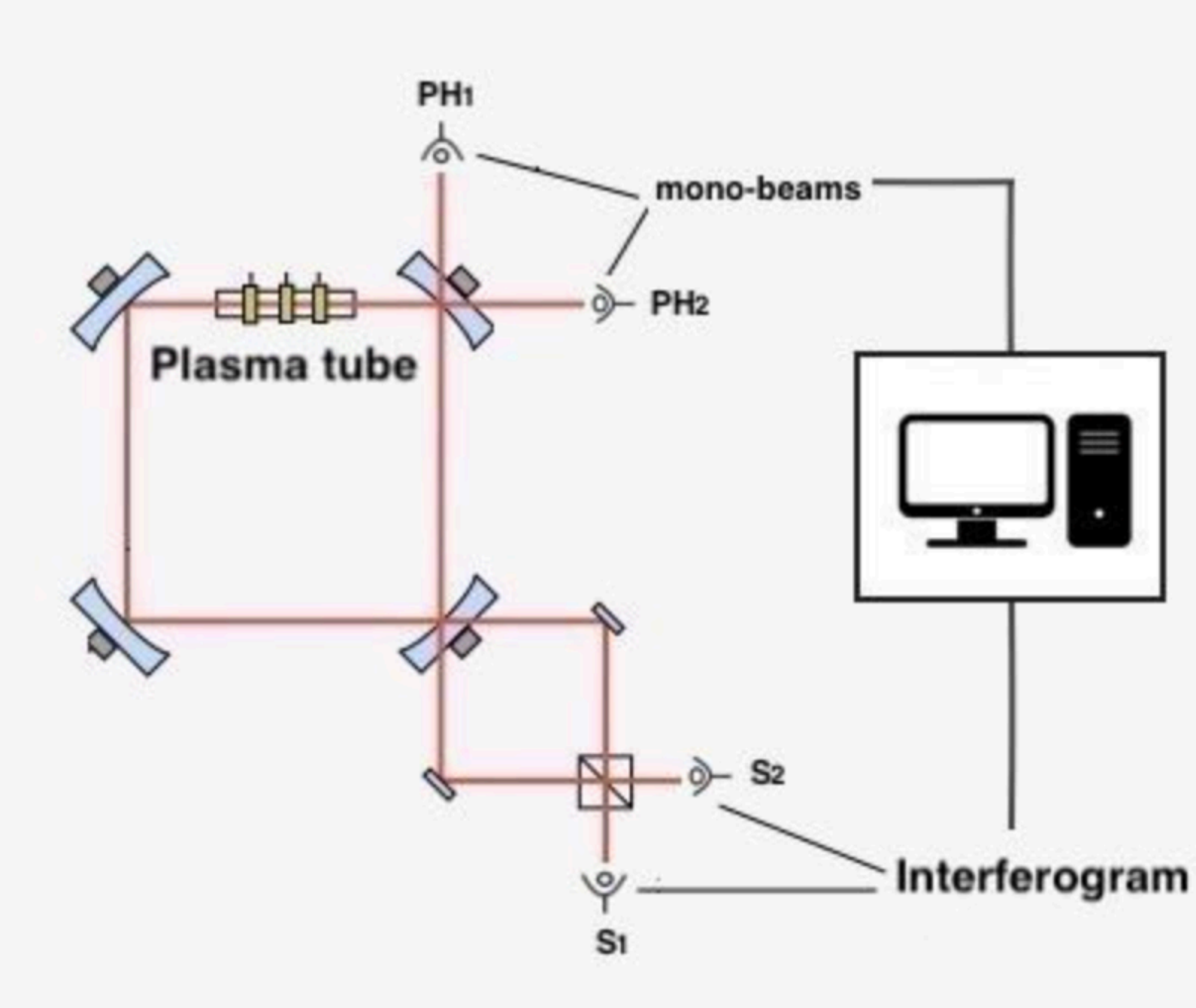

Since autumn 2022, two beat note signals are acquired by GINGERino, "S1" and "S2".

- The 2 signals are in phase opposition
- The "difference" signal is used to evaluate the Sagnac frequency
- Detected power is doubled
- The signal-to-noise ratio is expected to be enhanced by a factor $\sqrt{2}$
- Common mode disturbances are cancelled

New quantities available for diagnostics:

- ***First products:*** ω_{s01}, ω_{s02} , ω_{s0S} ***(the latter is the difference between the first two, in phase opposition)***
- ***The quantity "resto" :*** ω_{s01}-ω_{s02}
- ϵ_1***: phase difference between the 2 beat note signals***

Diagnostics: timing precision of Gingerino DAQ systems

Simulations:

- **Simulations of time jitter noise** have been produced, by **adding a random noise δt to ideal time intervals**
- By **injecting such noise in an ideal beat note signal**, it was possible to obtain a **linear relationship** between the standard deviation of the ideal ω_m disturbed by the time jitter and the standard deviation of the time jitter:

$$std(\omega_m) = k_{jit} \cdot std(\delta t), \quad k_{jit} \sim 0.38 \frac{mHz}{\mu s}$$

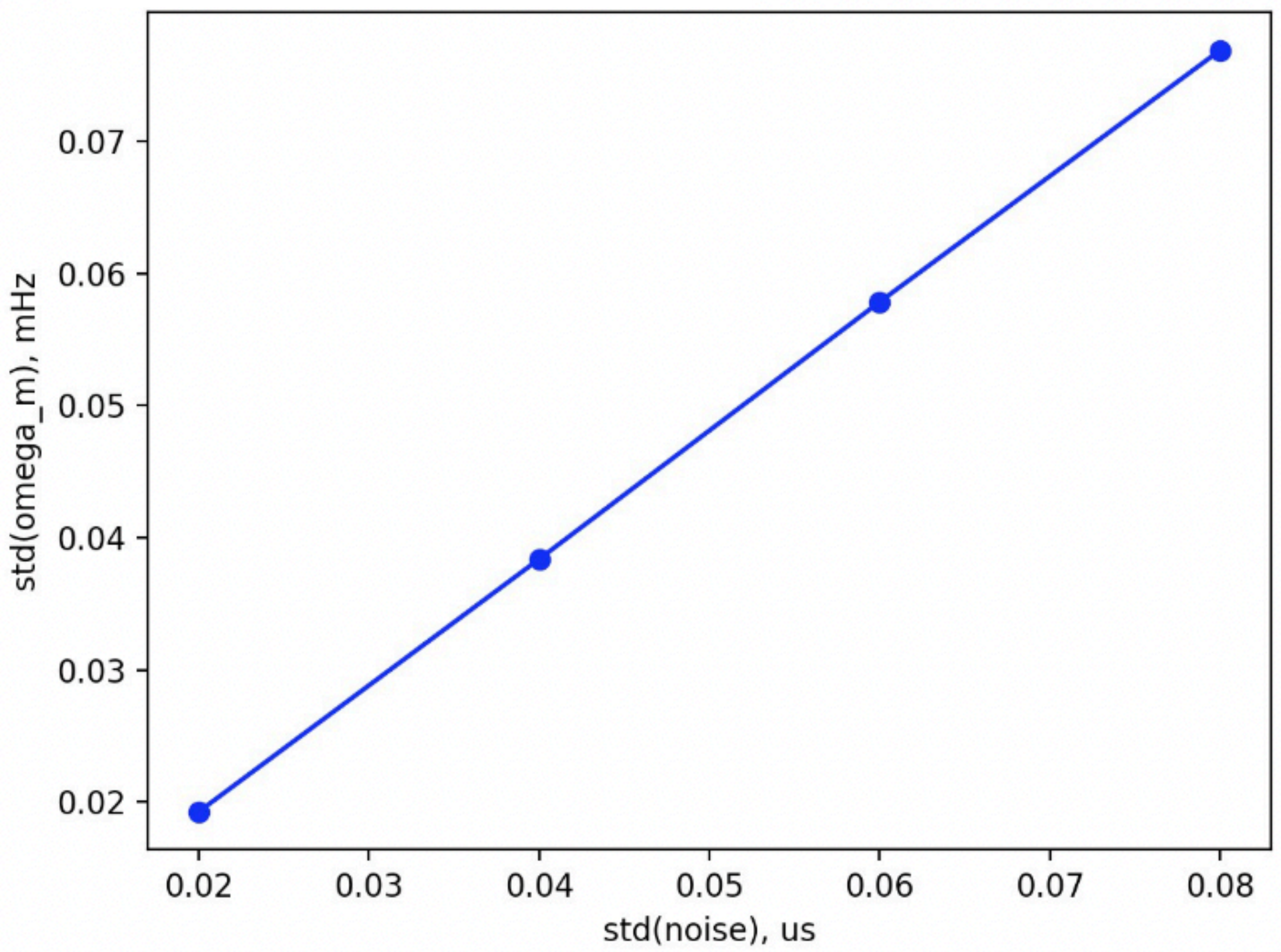

Evaluation of upper limits

Subtraction of same ω_m signal from PXI and Centaur

- Interpretation of the residual as due to time jitter, and evaluation of upper limits, for PXI and Centaur
- data from PXI and Centaur are synchronized with cross-correlation and then subtracted

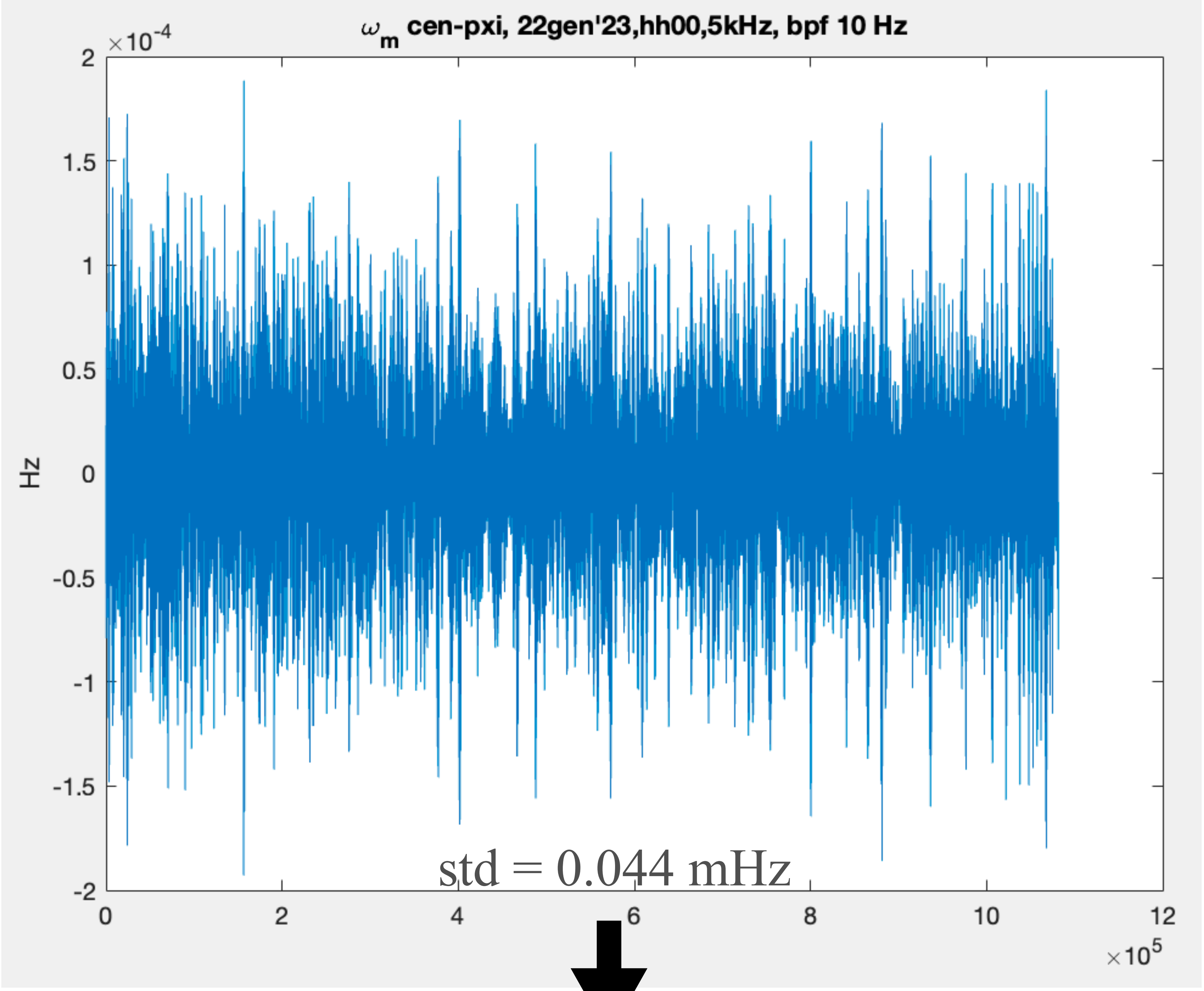

Upper limit on time jitter noise: 0.046 μs/200 μs (PXI), or 0.12μs/500μs (Centaur)

Such result stays unchanged if evaluated using the double beat note signal

Conclusions and perspectives:

Data for seismology from 2016 will be available on EIDA, ω_{s0} , 100 Hz

A plugin will be implemented for real time data on EIDA

We have capability to characterize a RLG: planarity, alignment, polarization state of the beams, and improve the quality of the interference

From the availability of a double beat note signal, the implementation of a more advanced and stable data selection is in progress

Measuring time precision issues led to the decision of utilizing a Rb clock, that was installed on Gingerino acquisition by Paolo Marsili and will be in operation in the very next future

New achievements in hardware and analysis are in view of the upgrade to Ginger